電気学会論文誌●（●●●●●●●部門誌）
IEEJ Transactions on ●●●●●●●●●●●●●●●●
Vol.●● No.● pp.●-● DOI: ●.●●/ieejeiss.●●.●

Paper

Damping Control of Filter Resonance Focusing on Output Stage for Multi-Modular Matrix Converter

Hiroki Takahashi*, Student member, Jun-ichi Itoh*a), Member

(Manuscript received Jan. 00, 20XX, revised May 00, 20XX)

This paper discusses a damping control that is applied to multi-modular matrix converters in order to suppress the oscillation due to the LC resonance of the input filter. The multi-modular matrix converter connects a multiple winding transformer and several modules. The module consists of a three-phase to single-phase matrix converter and filter capacitors. It is found that the multi-modular matrix converter has a resonance problem between the leakage inductance of the transformer and the filter capacitors in the modules. In this paper, a damping control combined with the output current control of the multi-modular matrix converter is proposed to suppress the resonance and to achieve better input current quality. The proposed damping control can divert the output current sensors for an ACR (auto current regulator), which is generally used in the adjustable speed drive system of a motor. Therefore, the proposed damping control does not require additional sensors, which is an advantage over the conventional damping control applied to the input stage of the multi-modular matrix converter. From the experimental results, the proposed damping control improves the input current THD (total harmonic distortion) by 75.5%. In addition, the proposed damping control obtains a higher damping performance than the conventional damping control.

Keywords : multi-modular matrix converter, filter resonance, damping control, high power conversion

1. Introduction

Recently, matrix converters have attracted a lot of attentions among the researchers because this converter has no DC energy buffer such as bulky electrolytic capacitors [1]-[7]. Matrix converters promise to achieve higher efficiency, smaller size and longer life-time compared to the conventional BTB (back to back) system which consists of a PWM (pulse width modulation) rectifier and a PWM inverter. In addition, matrix converters achieve bidirectional power flow, unity input power factor, and sinusoidal input and output waveforms.

In order to utilize these advantages of matrix converters for high power applications, such as wind turbines, pumps and blowers, the multi-modular matrix converters are investigated [8]-[10]. The multi-modular matrix converter consists of several modules of three-phase to single-phase matrix converter and a multiple winding transformer. The multiple winding transformer is placed between a power grid and matrix converter modules, and output terminals of each module are connected in series or parallel in order to provide high voltage or high power. The advantages of this modular structure with the multiple winding transformer are following: 1) the circuit structure, especially placement of devices in the modules, is simple; 2) special modulation schemes to prevent the interference between the connected modules are not required because the transformer isolates each module. Consequently, high power conversion systems employing a matrix converter topology can be designed and provided easily with the conventional modulation schemes.

The multi-modular matrix converter requires LC filters in the input side to eliminate the harmonic current due to the switching operation and to assist in the commutation similarly to general matrix converters. Besides, the multi-modular matrix converter uses the filter capacitors in the matrix converter modules only because the leakage inductance of the transformer can be treated as the filter inductors. Nevertheless, if the LC resonance occurs between the leakage inductance and the input filter capacitors, the resonance results in substantial distortions in the input current. A general solution to the problem of resonance in general matrix converters is to connect damping resistors in parallel with the input filter inductors [11]. However, in the multi-modular matrix converter, the damping resistors cannot be connected in parallel with the leakage inductance of the transformer, practically.

One of other solution to suppress the resonance is to connect the damping resistors in series with the input filter capacitors. However, this method results in more losses in the damping resistors due to the harmonic current caused by switching operation in comparison with the former method [12]. Hence, the solution using a special control to suppress the resonance is necessary.

In the controls to suppress the filter resonance, active damping controls for current source converters and general matrix converters have been proposed [13]-[18]. These methods suppress the resonance with virtual damping resistors in parallel with filter capacitors based on the input current control of the converters. In this paper, this active damping control based on the input current control is defined as the conventional damping control. If the conventional damping control is applied to the multi-modular matrix converter, the additional voltage sensors for the conventional damping control are required. Furthermore, the number of the voltage sensor depends on the number of modules. This increase of the voltage sensors is not cost effective. In addition, if the multi-modular matrix converter also employs the output current control with a feedback (ACR: auto current

a) Correspondence to: Jun-ichi Itoh. E-mail: itoh@vos.nagaokaut.ac.jp
* Nagaoka University of Technology
1603-1, Kamitomioka-cho, Nagaoka, Niigata, Japan 940-2188

regulator) for the field oriented control, the converter has several feedback loops in both of the input and output stages. This means that the conventional damping control interferes with the output current control through the converter. Hence, the design method of the conventional damping control and the output current control may be complicated.

On the other hand, the damping control combined with the output current control of a general matrix converter was suggested [19]. This method can achieve not only the resonant suppression but also the output current control at a same time. And the input current is fed by an open-loop control. However, the validity of the damping control combined with the output stage for the multi-modular matrix converter has not been clarified.

In this paper, the damping control that is combined with the output current control of the multi-modular matrix converter is proposed. The proposed damping control suppresses the filter resonance and also diverts the output current sensors for the ACR, which is generally used in the field oriented control, instead of using voltage sensors on the input stage. Firstly, the mechanism of the filter resonance is clarified in this paper. Secondly, the proposed damping control is discussed with the control block diagrams and its features. Thirdly, the validity of the proposed damping control for the multi-modular matrix converter is confirmed by simulation and experimental results. Finally, the compared results of damping effect between the proposed damping control and the conventional damping control is evaluated, experimentally.

2. Multi-modular Matrix Converter

2.1 System Configuration Fig. 1 shows the system configuration of a series multi-modular matrix converter with nine modules as shown in [8]-[10]. The series topology outputs 7-level high voltage which results in low harmonic components. The multiple winding transformer is located between the power source and the matrix converter modules. The transformer cancels the low order harmonics in the primary current of the transformer and reduces the ripples in the output voltage owing to phase shift of the secondary windings by 20 degrees.

Fig. 2 shows a simple model of a multi-modular matrix converter with three modules for analysis and consideration. In Fig. 2, each module consists of a three-phase to single-phase matrix converter and filter capacitors. The bidirectional switch in the modules uses 2 series-connected IGBT-diode. The filter capacitor C_f is connected closely with the bidirectional switches to mitigate surge voltage to the switches. An output terminal p is connected to load and another terminal n forms the neutral point with other modules.

2.2 Mechanism of Filter Resonance Fig. 3 shows the single-phase equivalent circuit of the input filter of the multi-modular matrix converter as illustrated in Fig. 2. In Fig. 3, L_l is the leakage inductance of the transformer and C_{fp} is the equivalent filter capacitor. L_l and C_{fp}, are converted to the primary side of the transformer. Thus, the equivalent capacitance C_{fp} is represented by the following equation.

$$C_{fp} = n\left(\frac{V_2}{V_1}\right)^2 C_f \quad \text{..... (1)}$$

where, n is the number of the modules and V_2/V_1 is the voltage transformation ratio of the transformer. In addition, v_p is the source voltage and i_{mc} is the current controlled by the modules.

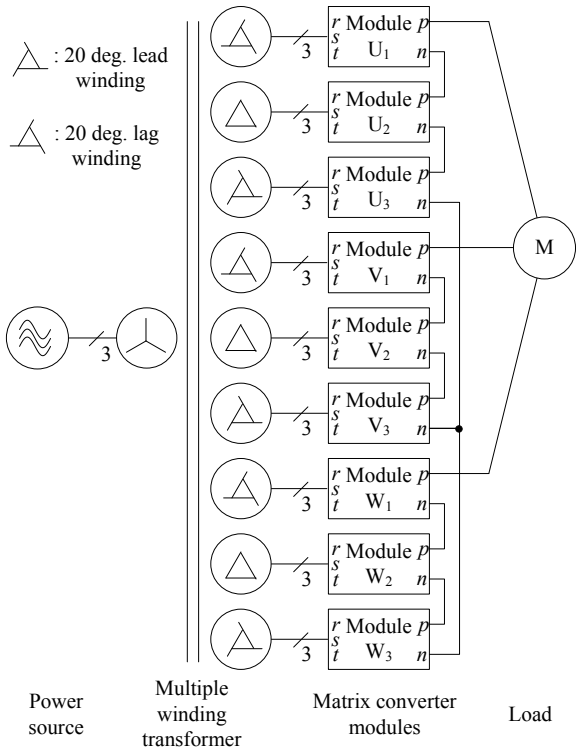

Fig. 1. System configuration of a series multi-modular matrix converter with nine modules.

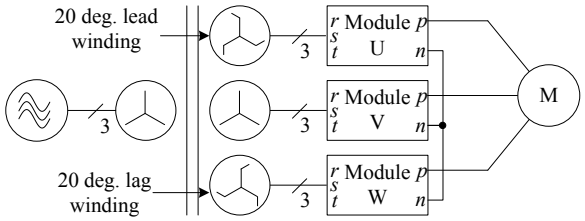

(a) System configuration.

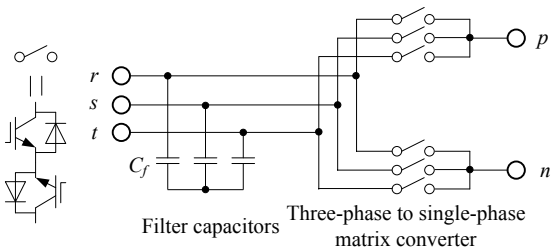

(b) Configuration of a matrix converter module.

Fig. 2. Simple model of a multi-modular matrix converter with three modules.

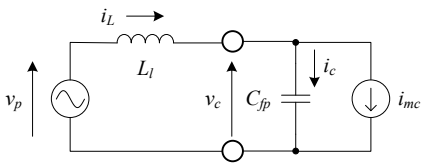

Fig. 3. Single-phase equivalent circuit of the input filter in the multi-modular matrix converter.

Note that the amplitude of i_{mc} is decided by the load power. The input power factor is assumed to unity. The exciting inductance of the transformer is assumed to be much larger than the leakage inductance for the simplicity.

The secondary current of the transformer includes the harmonic components caused by the power pulsation due to the single-phase output configuration of the module. The frequencies of these harmonics are expressed by the following equations.

$$f_{2d1} = \left| f_{in} - 2f_{out} \right| \quad \text{..... (2)}$$

$$f_{2d2} = \left| f_{in} + 2f_{out} \right| \quad \text{..... (3)}$$

where, f_{2d1} and f_{2d2} are the frequencies of the harmonics in the secondary current, f_{in} is the frequency of the power source and f_{out} is the output frequency. However, the primary current of the transformer i_L is a sinusoidal waveform because the harmonic components expressed from (2) to (3) are canceled by the multiple winding transformer.

The filter resonance occurs because of an equivalent negative resistor which is virtually generated at a constant power load. The mechanism to generate the equivalent negative resistor will be described as follows.

First of all, the filter capacitor voltage v_c, the input current of multi-modular matrix converter i_{mc} and the output power p_{mc} are defined as follows.

$$v_c = v_{cs} + \Delta v_c \quad \text{..... (4)}$$

$$i_{mc} = i_{mcs} + \Delta i_{mc} \quad \text{..... (5)}$$

$$p_{mc} = p_{mcs} + \Delta p_{mc} \quad \text{..... (6)}$$

where, suffix "s" represents steady components based on the voltage source angular frequency ω_{in} whereas suffix "Δ" means differential components in transient state. Then, the steady components are expressed from (7) to (10).

$$v_{cs} = \sqrt{2} V_c \cos \omega_{in} t \quad \text{..... (7)}$$

$$i_{mcs} = \sqrt{2} I_{mc} \cos \omega_{in} t \quad \text{..... (8)}$$

$$p_{mcs} = v_{cs} i_{mcs} = V_c I_{mc} \left(1 + \cos 2\omega_{in} t \right) \quad \text{..... (9)}$$

$$R_{mcs} = \frac{v_{cs}}{i_{mcs}} = \frac{V_c}{I_{mc}} \quad \text{..... (10)}$$

where, V_c and I_{mc} are the RMS values of the filter capacitor voltage and the input current of the multi-modular matrix converter, and R_{mcs} is an equivalent resistor defined as an impedance model of the multi-modular matrix converter. Note that the output power of the single-phase model oscillates with the frequency by twice of ω_{in} though the output power of the three phase model is constant.

From (4) to (6), i_{mc} is represented by (11).

$$i_{mc} = \frac{p_{mc}}{v_c} \quad \text{.....(11)}$$

Equation (11) is applied the linear approximation method around the operating point in steady state because (11) is a nonlinear equation. The input current i_{mc} is separated into steady and differential components and they are expressed as (12) and (13), respectively.

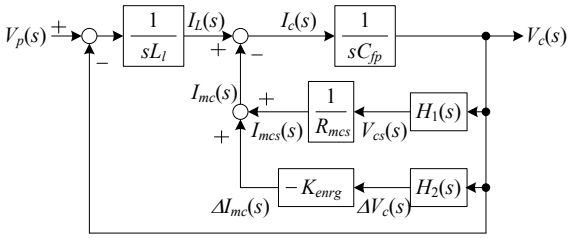

Fig. 4. Block diagram of the single-phase equivalent circuit of the input filter at a constant load.

$$i_{mcs} = \frac{p_{mcs}}{v_{cs}} = \frac{1}{R_{mcs}} v_{cs} \quad \text{..... (12)}$$

$$\Delta i_{mc} = \frac{\Delta p_{mc} - \Delta v_c i_{mcs}}{v_{cs}} \quad \text{..... (13)}$$

For a constant load, (14) is derived because Δp_{mc} becomes zero.

$$\Delta i_{mc} = -\frac{i_{mcs}}{v_{cs}} \Delta v_c = -K_{enrg} \Delta v_c \quad \text{..... (14)}$$

where, K_{enrg} is an equivalent negative resistor gain. Equation (14) indicates the fluctuation of the input current of the multi-modular matrix converter against the fluctuation of the filter capacitor voltage. In other words, an equivalent negative resistor is generated at a constant power control, which is obvious because the coefficient of Δv_c is a negative value.

Fig. 4 shows the block diagram of the single-phase equivalent circuit of the input filter in the multi-modular matrix converter at a constant load. In order to separate the steady and differential components, filters named $H_1(s)$ and $H_2(s)$ are introduced. $H_1(s)$ and $H_2(s)$ are a LPF (Low Pass Filter) and a HPF (High Pass Filter) respectively, and defined by (15).

$$H_1(s) + H_2(s) = 1 \quad \text{..... (15)}$$

Fig. 4 has a positive feedback loop because of the negative resistor gain -K_{enrg}. As a result, this system becomes unstable with LC resonance. This is also obvious from the transfer function of Fig. 4 presented from the following equation.

$$\frac{V_c(s)}{V_p(s)} = \frac{\dfrac{1}{L_l C_{fp}}}{s^2 + \dfrac{1}{C_{fp}} \left(\dfrac{1}{R_{mcs}} H_1(s) - K_{enrg} H_2(s) \right) s + \dfrac{1}{L_l C_{fp}}} \quad \text{..... (16)}$$

$H_1(s)$ passes the steady component in the filter capacitor voltage based on the angular frequency ω_{in}. On the other hand, in a transient state disturbed from the output stage, the filter capacitor voltage fluctuates with the resonant frequency because the capacitor is charged from the power source through the leakage inductance. Then, $H_2(s)$ passes the resonant component whose frequency is generally over 10 times as large as the fundamental frequency. Thus, $H_2(s)$ can be assumed as 1 in this resonant frequency region and (17) is obtained. However, the full analysis about this issue is a future work whereas this paper discusses the filters on the separated frequency bandwidth for simplicity.

$$\frac{\Delta V_c(s)}{\Delta V_p(s)} = \frac{\dfrac{1}{L_l C_{fp}}}{s^2 - \dfrac{K_{enrg}}{C_{fp}} s + \dfrac{1}{L_l C_{fp}}} \quad \text{..... (17)}$$

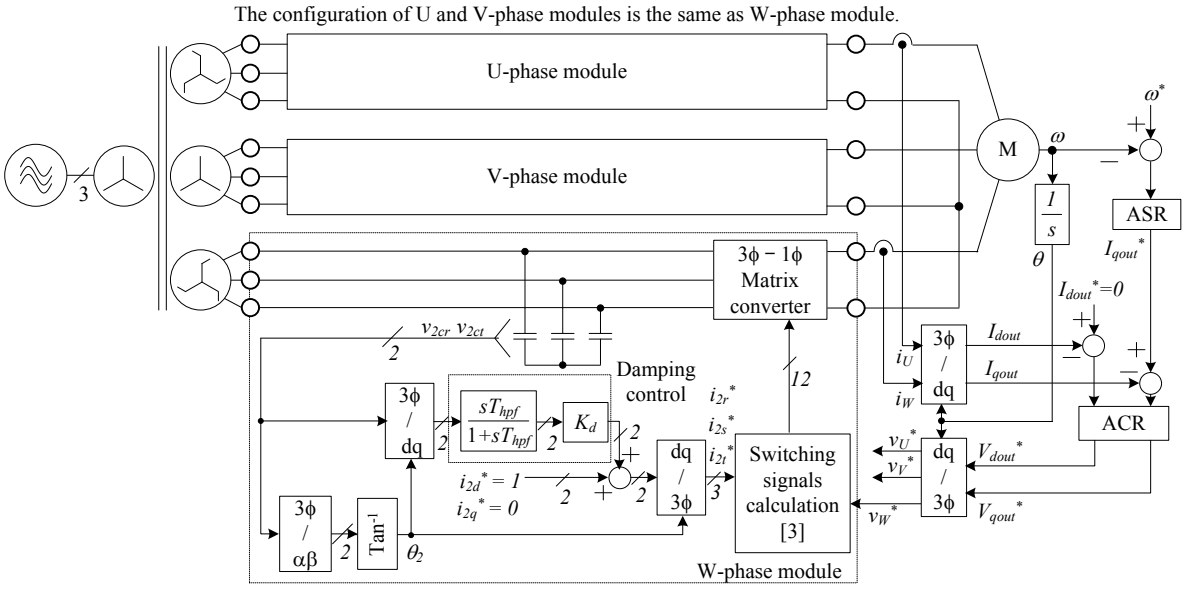

Fig. 5. Control block diagram of the multi-modular matrix converter employing the conventional active damping control.

This equation indicates the damping factor of the system becomes negative and this characteristic appears strictly when the fast feedback control is applied to the output stage of the multi-modular matrix converter [20]. A typical feedback control in an adjustable speed drive system of a motor is the field oriented control including an ACR as a minor loop. The field oriented control is necessary for industry. However, for the multi-modular matrix converter, the fast output current control in the field oriented control behaves as the equivalent negative resistor. Therefore, the multi-modular matrix converter must cancel the negative resistor gain in Fig. 4 with its control strategy when the output current control is applied.

3. Control Strategy to Suppress Filter Resonance

Fig. 5 shows the control block diagram of the multi-modular matrix converter employing the conventional active damping control. The basic concept of this technique is to insert a virtual harmonic damping resistor in parallel with the filter capacitor C_f owing to the input current control in Fig. 5. As a result, the virtual harmonic damping resistor cancels the negative resistor gain with no influence on the fundamental component. However, the active damping control requires high speed response and high accurate voltage sensors in order to detect high frequency harmonic components. In addition, the required voltage sensors are increased with the number of modules. For example, the multi-modular matrix converter with nine modules as shown in Fig. 1 needs 18 voltage sensors at least for the active damping control. Therefore, the damping control which is independent from the number of modules is preferred.

In addition, the multi-modular matrix converter has two feedback loops in both of the input and output stages because of the conventional active damping control and the ACR for the output current included in a field oriented control. This means that the design method of the conventional damping control and the output current control may be complicated. Hence, the damping control which is applied to the output stage is preferred.

In order to overcome these issues, the damping control combined with the output current control of the multi-modular matrix converter is proposed. The proposed method diverts the current sensors for the ACR and does not require the voltage sensors at the filter capacitors. Thus, the required sensors for the proposed damping control are independent from the number of modules. Furthermore, the design of controllers for the ACR and the damping control are simpler than the conventional method because the feedback loop is applied to the output stage only.

Fig. 6 shows the system block diagram of the multi-modular matrix converter with the proposed damping control. The output voltage control block includes the proposed damping control to suppress the input filter resonance, and a field oriented control composed of the ACR and the ASR (auto speed regulator). On the other hand, the secondary current of the transformer is fed by an open-loop control. The secondary voltage phase angles of the transformer of U-phase and V-phase modules, θ_{2U} and θ_{2V}, are calculated from (18) to (19) using the secondary voltage phase angle of W-phase module θ_{2W}.

$$\theta_{2U} = \theta_{2W} + 2\pi/9 \text{ [rad]} \quad (18)$$

$$\theta_{2V} = \theta_{2W} + \pi/9 \text{ [rad]} \quad (19)$$

Note that this voltage detection is required to one module only and this detection is independent from the number of modules.

Next, this paragraph explains the output voltage control block. First of all, a HPF which has a time constant T_{hpf} separates the harmonic components caused by the filter resonance from the output current, I_{dout} and I_{qout}. This is based on the principle that the resonant distortion appears in the output current since the matrix converters has no energy buffer. The cut-off frequency of the HPF is set lower than the resonant frequency because the fundamental frequency component in the output current is converted to a constant value by a synchronous reference frame. Besides, the harmonic components are converted to ripples. The extracted ripples are multiplied by the damping gain K_d, and subtracted from the output current. The above shows the theory of the damping control in order to suppress the resonant distortion. On the other hand, the output current is controlled by the ACR for the deviation obtained from the output current commands I_{dout}^* and I_{qout}^*, and

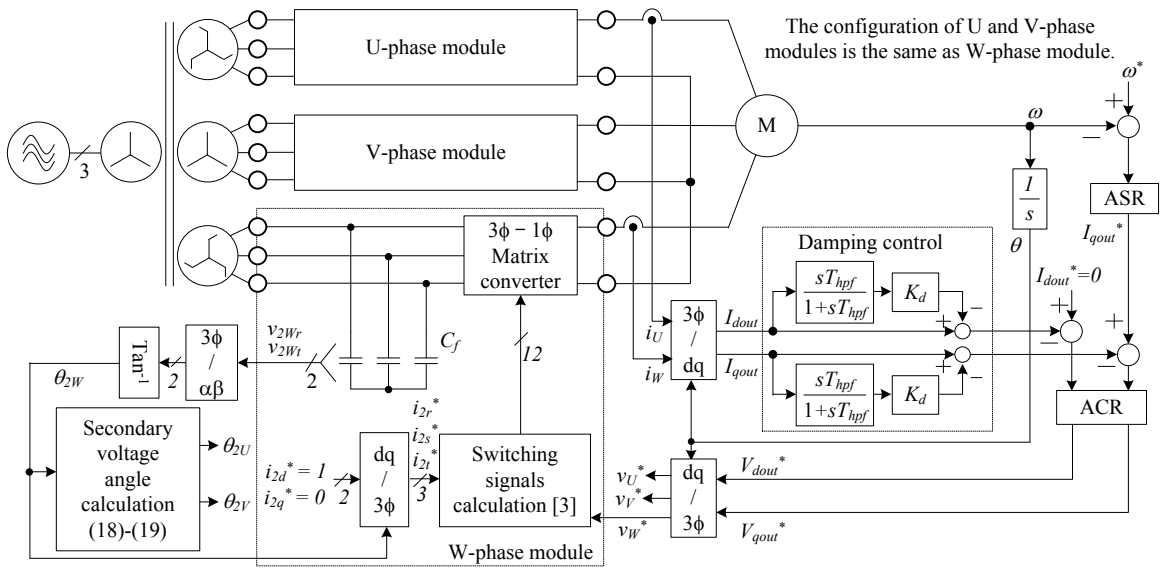

Fig. 6. Control block diagram of the multi-modular matrix converter with the proposed damping control.

feedback values from the damping control. As a result, the damping control path in Fig. 6 becomes positive feedback eventually.

Fig. 7 shows the block diagram of the single-phase equivalent circuit of the input filter with the conventional and the proposed damping controls. K_{io} is defined as the following equation.

$$K_{io} = \frac{1}{\lambda R_{mcs}} \frac{V_2}{V_1} \quad \text{..... (20)}$$

where, λ is the modulation index of the multi-modular matrix converter at steady state and K_{io} is a coefficient to connect the input stage and the output stage of the multi-modular matrix converter. In addition, in Fig. 7 (a), $V_{c2}(s)$ is the filter capacitor voltage converted to the secondary side of the transformer, $\Delta I_{mcd}(s)$ and $\Delta I_{mcd2}(s)$ are the compensated primary and secondary current of the transformer owing to the damping control. In contrast, in Fig. 7 (b), I_{out}(s) is the output current, ΔI_{outd}(s) is the output of the damping control, ΔV_{outd}(s) and ΔV_{outd_m}(s) are the compensated output voltages of the system and the module owing to the damping control. As discussed in section 2.2, the filter resonance is excited by the fast feedback control for the output current. In other words, the behavior of the input current of the module affected by the output current control generates the equivalent negative resistor gain. In the conventional damping control as illustrated in Fig. 7 (a), the damping control path containing the damping HPF and the damping gain K_d is added to the block diagram. This is because the damping compensation current ΔI_{mcd}(s) is obtained by the detection of the filter capacitor voltage and is added to the input current command i_{2d}^* and i_{2q}^* in Fig. 5. On the other hand, if the proposed damping control is introduced as shown in Fig. 6, the output voltage command is separated to the component generating the equivalent negative resistor gain and the damping compensation voltage ΔV_{outd}(s). This is equivalent to adding the damping path to the block diagram such as the conventional method. Thus, the damping path in Fig. 7 (b) contains the parameters on the output stage and K_{io}. The transfer function of Fig. 7 (b) focusing on the frequency range which the damping HPF and $H_2(s)$ are assumed as 1 is presented as following.

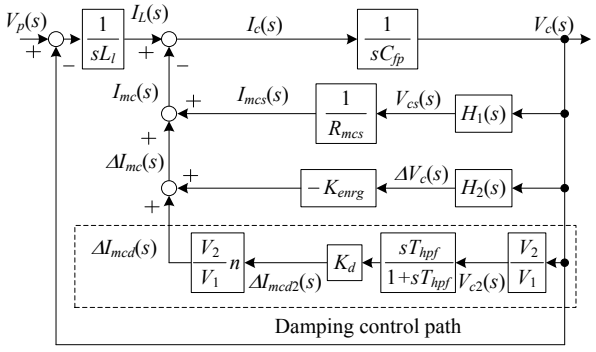

(a) With the conventional damping control.

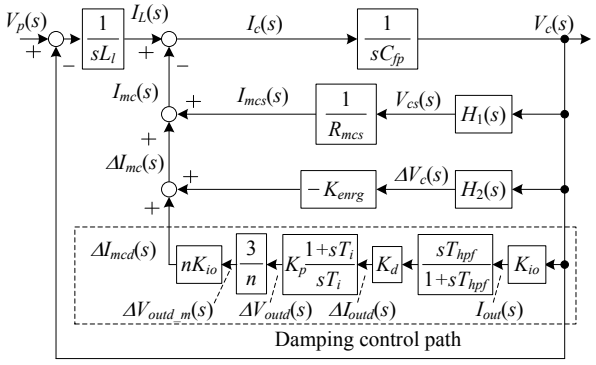

(b) With the proposed damping control.

Fig. 7. Block diagram of the single-phase equivalent circuit of the input filter in the multi-modular matrix converter with the damping controls.

$$\frac{\Delta V_c(s)}{\Delta V_p(s)} = \frac{\frac{1}{L_l C_{fp}}}{s^2 + \frac{1}{C_{fp}}\left(K - K_{enrg}\right)s + \frac{1}{C_{fp}}\left(\frac{1}{L_l} + \frac{K}{T_i}\right)} \quad \text{..... (21)}$$

$$K = 3K_{io}^{\ 2} K_d K_p \quad \text{..... (22)}$$

Therefore, the proposed damping control maintains the positive

Table 1. Simulation conditions.

(a) Common conditions.

Input line voltage	200 V_{rms}	ASR natural frequency	63.7 Hz
Input frequency	50 Hz	ACR natural frequency	650 Hz
Rated power	3 kW	Carrier frequency	10 kHz
Leakage inductance	9.42 %	Damping HPF cut off frequency	30 Hz
Input filter C	8.55 %		

(b) Conditions depending on the number of modules.

	3-module model	9-module model
Voltage transformation ratio V_2/V_1	1	1/3
Damping gain	0.6 p.u.	0.55 p.u.

Table 2. IPM motor parameters.

Rated speed	1800 rpm (1 p.u.)
Rated line voltage	180 V_{rms}
Rated power	1.5 kW
Rated current	6.1 A_{rms} (1 p.u.)
d-axis inductance	11.5 mH
q-axis inductance	23.0 mH
Stator resistance	0.783 Ω
Inertia moment	0.00255 kgm^2

damping factor and suppresses the filter resonance.

4. Simulation Results

Table 1 presents simulation conditions for the multi-modular matrix converter with three modules as drawn in Fig. 2 and nine modules as shown in Fig. 1. The simulations are tested with a field oriented control which is composed of the ASR and the ACR to control rotation speed of the IPM (interior permanent magnet) motor. The negative resistor appears because the ACR keeps constant output power in the motor load. In addition, note that the filter inductors are added in the primary side instead of the large leakage inductance of the transformer. On the other hand, Table 2 shows the IPM motor parameters as the load in the simulation.

4.1 Three-module model Fig. 8 shows the input and output waveforms of the three-module model of the multi-modular matrix converter at steady state in simulations. Note that these results are obtained when the IPM motor operates at rated speed and rated torque output. Fig. 8 (a) shows the result without damping controls and (b) shows the result with the proposed damping control. It can be confirmed that the primary current of the transformer contains large distortion caused by the filter resonance from Fig. 8 (a), and the primary current THD (total harmonic distortion) is 62.9%. Moreover, the output line voltage and the output current have large distortion too because matrix converter modules have no energy buffers. The output current THD is 15.4% from Fig. 8 (a). On the other hand, in Fig. 8 (b), the resonant distortion in the output current is mitigated by the proposed damping control. As a result, the primary current of the transformer contains less distortion compared to Fig. 8 (a). Both the primary current of the transformer and the output current THDs are under 1% in Fig. 8 (b). In addition, the output line voltage obtains 5- level waveform.

Fig. 9 shows the transient waveforms regarding the IPM motor.

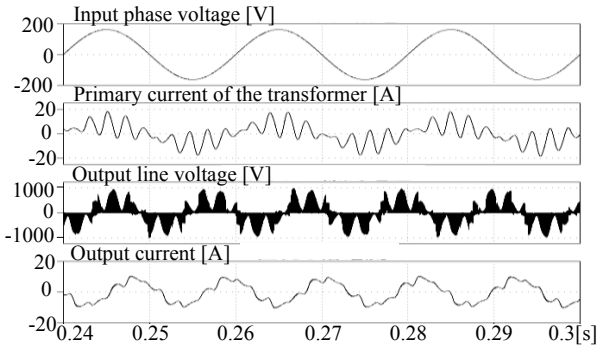

(a) Without damping controls which results in the primary current and the output current THDs by 62.9% and 15.4%, respectively.

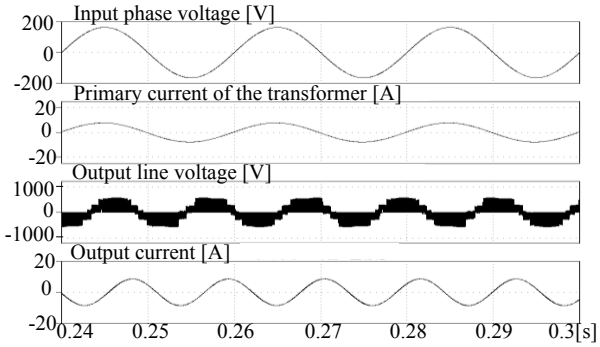

(b) With the proposed damping control which results in the primary current and the output current THDs under 1%.

Fig. 8. Input and output waveforms of the three-module model of the multi-modular matrix converter as drawn in Fig. 2 at steady state in simulations.

Fig. 9 (a) shows the result without damping controls and (b) shows the result with the proposed damping control. In Fig. 9 (a), the dq-axis currents and the output torque oscillate during acceleration period and at rated speed and rated torque output due to the filter resonance. On the other hand, in Fig. 9 (b), the current and torque oscillations are suppressed by the proposed damping control. However, the overshoot of the d-axis current by 1.2 p.u. occurs when the rated torque is provided although the d-axis current command is set to zero. This problem will be overcome by the optimal design of the controllers in future works. Therefore, it is confirmed from the simulation results that the proposed damping control suppresses the filter resonance and achieves stable operation with the IPM motor load.

4.2 Nine-module model Fig. 10 shows the input and output waveforms of the multi-modular matrix converter with nine modules. This simulation result clarifies that the proposed damping control is applicable to the practical multi-modular matrix converter. In common with the simulation of the three-module model, these results are obtained when the IPM motor operates at rated speed and rated torque output. Fig. 10 (a) shows the result without damping controls and (b) shows the result with the proposed damping control. From Fig. 10 (a), the primary current THD of the transformer and the output current THD are yielded by 72.9% and 18.6% respectively because of the filter resonance. However, from Fig. 10 (b), both of these currents contain less resonant distortion than the result of (a) owing to the proposed damping control. The primary current THD of the transformer is 1.77% and the output current THD is under 1%. In addition, the output line voltage waveform has multi-level like a

sinusoidal waveform. Therefore, it is confirmed that the proposed damping control is applicable to the multi-modular matrix converter with nine modules in common with the three-module model.

5. Experimental Results

5.1 Verification of the Proposed Damping Control

Table 3 presents experimental conditions for the multi-modular matrix converter with three modules drawn in Fig. 2 because of the experimental limitation and the experiment with nine modules is a future work. Note that the experiments are tested with a constant power load composed of a R-L load and the ACR, not an field oriented control. The negative resistor appears even if the R-L load is used instead of the motor because the ACR keeps the output power constant. In addition, the filter inductors are added in the primary side instead of the large leakage inductance of the transformer in common with the simulation condition. The commutation sequence of the semiconductor switches is determined by the direction of the output current, that is, it is also called the current type commutation.

Fig. 11 shows the input and output waveforms of the multi-modular matrix converter obtained by the experiments. Fig. 11 (a) shows the result without damping controls and (b) shows the result with the proposed damping control. In Fig. 11 (a), the filter resonance is excited, and the primary current of the transformer and the output current have resonant distortions. The primary current of the transformer and the output current THDs are obtained as follows, 18.6% and 6.56%. The current THDs measured from experiments are lower than the simulation results because loss of the transformer and the modules behave as damping resistors. In contrast, the filter resonance is suppressed by the proposed damping control in Fig. 11 (b). Consequently, the primary current of the transformer and the output current obtain lower distortion compared to Fig. 11 (a). The primary current of the transformer and the output current THDs are 4.55% and 2.89%, respectively. Thus, the proposed damping control mitigates the resonance distortions by 75.5%. Furthermore, the output line voltage obtains 5-level waveform without the voltage fluctuation due to the filter resonance.

Fig. 12 shows the harmonic components analysis of the primary current of the transformer. Fig. 12 (a) shows the result without the proposed damping control and (b) shows the result with the proposed control. In Fig. 12 (a), the primary current of the transformer includes the 340-Hz and 440-Hz components by approximately 10% caused by the filter resonance. In contrast, in Fig. 12 (b), the resonant components are mitigated by the proposed damping control. In addition, the harmonic components within a range from 100 Hz to 1 kHz are suppressed by the proposed damping control since the proposed control has low cut-off HPF (30 Hz). This upper limit of suppressible harmonics is decided by the control bandwidth due to the control frequency. According to [18], the control delay due to the sampling and the PWM generation leads to the phase delay of the damping compensation command. The phase delay becomes 90 deg. when the resonant frequency is 1/8 of the control frequency in [18]. At this frequency, the damping control behaves as an inductance. This equivalent inductance cannot suppress the current distortion including the resonance. From this consideration, the proposed damping control suppresses the current distortion within 1.25 kHz in this experiment because the control frequency is set to 10 kHz

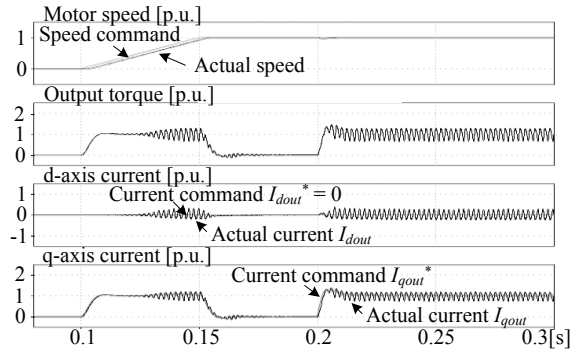

(a) Without damping controls which results in steady perturbation in the output torque and dq-axis currents due to the filter resonance.

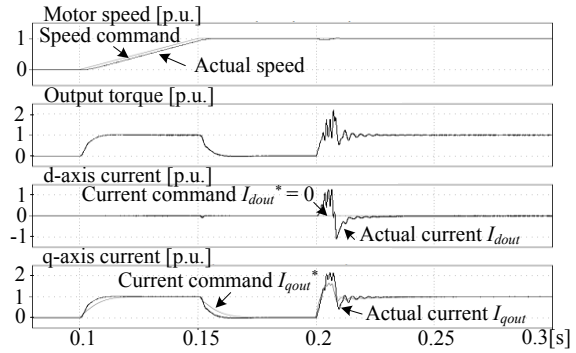

(b) With the proposed damping control which results in suppression of the steady fluctuation.

Fig. 9. Transient waveforms regarding the IPM motor.

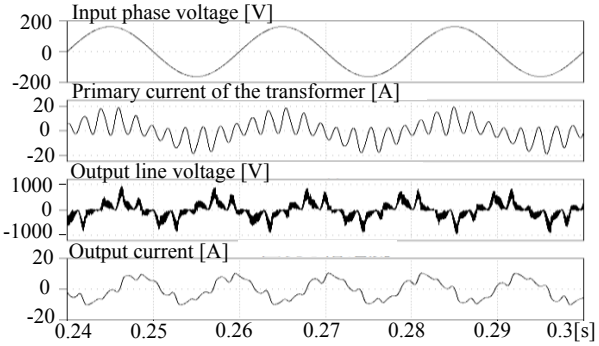

(a) Without damping controls which results in the primary current THD and the output current THD by 72.9% and 18.6%, respectively.

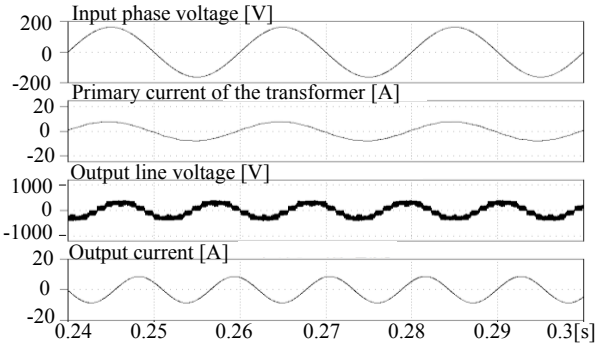

(b) With the proposed damping control which results in the primary current THD and the output current THD by 1.77% and under 1%, respectively.

Fig. 10. Input and output waveforms of the nine-module model of the multi-modular matrix converter as drawn in Fig. 1 at steady state in simulations.

Table 3. Experimental conditions.

Input line voltage	200 V_{rms}	Output frequency	30 Hz
Input frequency	50 Hz	Load resistance	83.7 %
Rated power	3 kW	Load inductance	1.88 %
Trans. turn ratio	1	ACR natural frequency	650 Hz
Leakage inductance	9.42 %	Load current command	0.95 p.u.
Input filter C	8.55 %	Damping gain	0.6 p.u.
Carrier frequency	10 kHz	Damping HPF cut off frequency	30 Hz
Commutation time	2.5 μs		

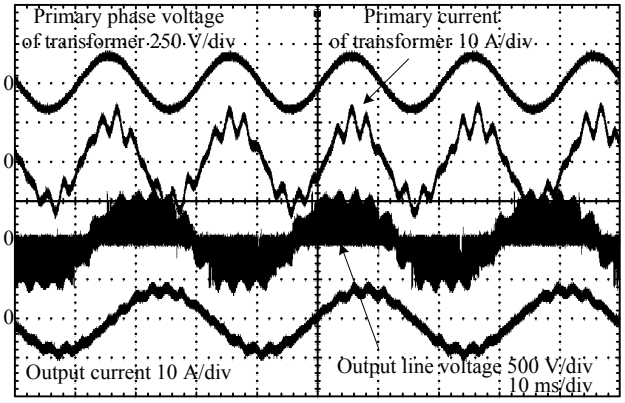

(a) Without damping controls which results in the primary current THD and the output current THD by 18.6% and 6.56%, respectively.

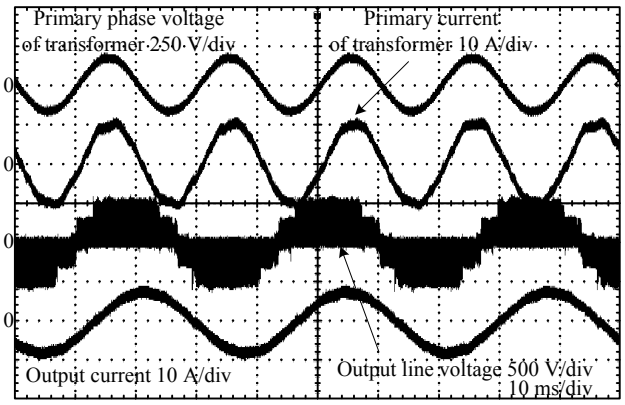

(b) With the proposed damping control which results in the primary current THD and the output current THD by 4.55% and 2.89%.

Fig. 11. Input and output waveforms of the multi-modular matrix converter with three modules in experiments.

same as the carrier frequency. However, the full consideration about this issue has to be reported in the future.

Fig. 13 shows the input and output waveforms of a module obtained from experiments. Fig. 13 (a) shows the waveforms without any damping controls and (b) shows the results with the proposed damping control. In Fig. 13 (a), the filter resonance generates distortion in the filter capacitor voltage and the secondary current of the transformer. However, in Fig. 13 (b), the resonant distortion in the filter capacitor voltage and the secondary current waveforms are suppressed by the proposed damping control. The secondary current THDs of transformer without and with the proposed damping control are 27.5% and 5.19%, respectively. Note that the secondary current THD calculation omits the power pulsation components expressed from (2) to (3). Furthermore, the filter capacitor voltage THD is reduced from 10.7% to 2.19%. From these results, it is confirmed that the

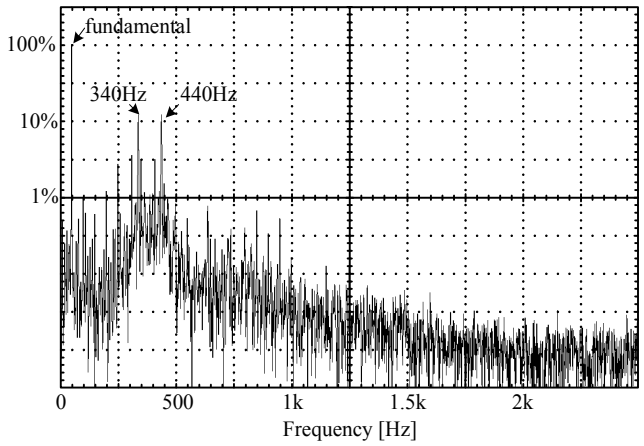

(a) Without damping controls.

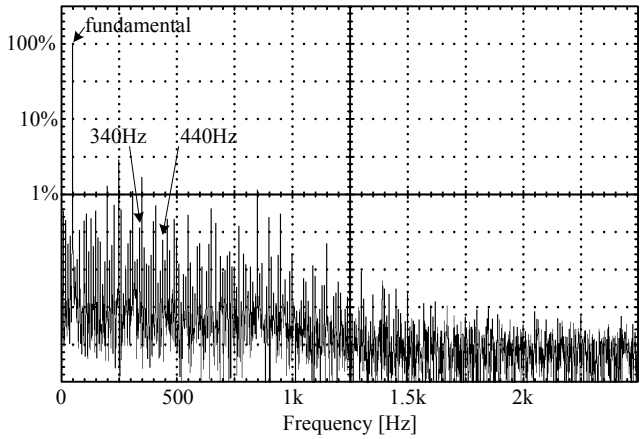

(b) With the proposed damping control.

Fig. 12. Spectrum of the primary current of the transformer with experiments.

proposed damping control suppresses the filter resonance and achieves stable operation.

5.2 Comparison with the Conventional Active Damping Method Applied to Multi-modular Matrix Converter

This section discusses the comparison between the conventional active damping control as drawn in Fig. 5 and the proposed damping control as illustrated in Fig. 6. This comparison results clarify the performance of the filter resonant suppression of each method. The evaluation subjects are the primary current THD characteristics against the output power and the leakage inductance of the transformer.

Fig. 14 shows the THD characteristics obtained from the primary current of the transformer which is subject to the output power. Note that the output line voltage is kept to 240 V_{rms} constantly. The damping gains of the conventional and the proposed damping controls are set to 1.0 p.u. and 0.6 p.u. respectively, and the cut-off frequency of the HPF in the damping controls is 30 Hz in common. Without any damping controls, the primary current THD of the transformer is increased to approximately 20% in the range over 60% of load due to the resonance. However, the conventional and proposed damping controls mitigate the primary current THD of the transformer. Then, the conventional control cannot reduce the primary current THD of the transformer and the primary current THD is approximately 10% in the range over 90% of load. On the other hand, the proposed damping control suppresses the THD under

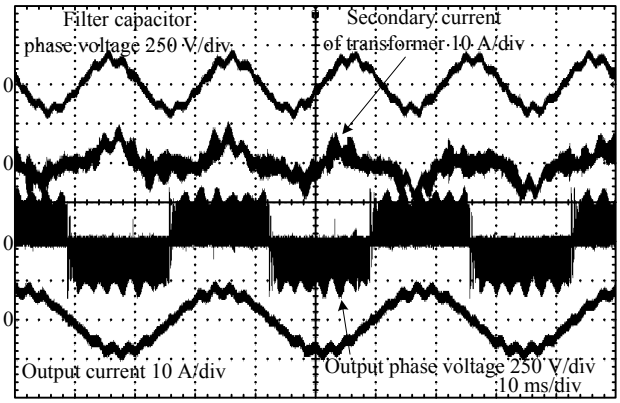

(a) With no damping controls which results in the capacitor voltage THD and the secondary current THD by 10.7% and 27.5%, respectively.

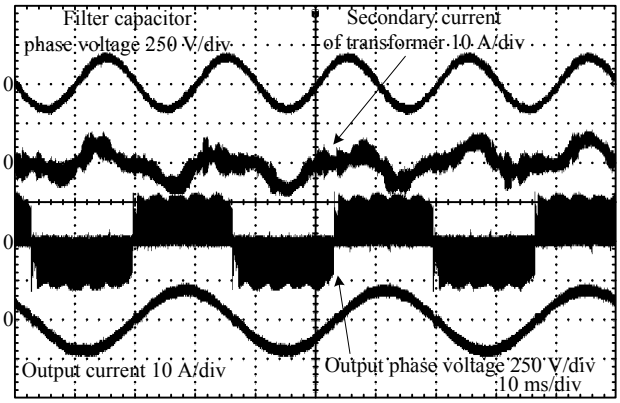

(b) With the proposed damping control which results in the capacitor voltage THD and the secondary current THD by 2.19% and 5.19%.

Fig. 13. Input and output waveforms of a module with experiment.

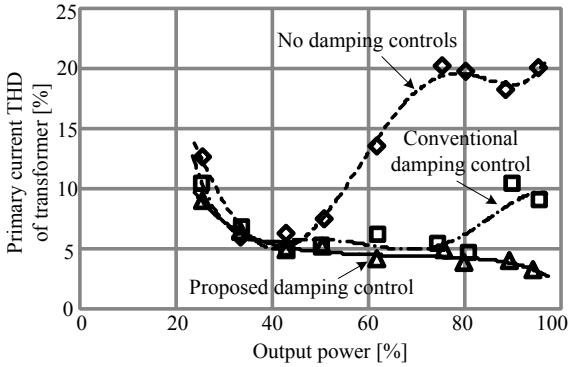

Fig. 14. THD characteristics obtained from the primary current of the transformer that is subject to the output power.

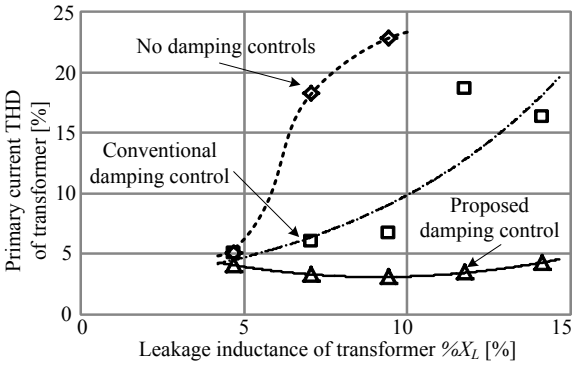

Fig. 15. THD characteristics of the primary current of the transformer that is subject to the leakage inductance of the transformer.

5% in the range more than 60% load. In the light load region especially under 40% load, the proposed damping control cannot reduce the primary current THD under 5%. The main reason of increasing THD is caused by the small amplitude of the fundamental component of the primary current although the distortion components are almost constant and unrelated to the load. This distortion is caused by the commutation failure, is not caused by the filter resonance. Thus, the proposed damping control suppresses the resonant distortion in larger range of the output power than the conventional damping control.

Fig. 15 shows the THD characteristics of the primary current of the transformer which is subject to the leakage inductance of the transformer. Without any damping controls, the primary current THD of the transformer increases with the leakage inductance. In particular, the data in the region over 10% of the leakage inductance of the transformer could not be taken because the primary current of the transformer diverges due to the destabilization. In contrast, the conventional and the proposed damping controls suppress the primary current THD. However, although the conventional damping control cannot suppress the primary current THD in the region over 9.42% of the leakage inductance, the proposed damping control mitigates the primary current THD under 5% in the condition of the leakage inductance from 4.71% to 14.1%. Hence, the proposed damping control mitigates the resonant distortion in larger range of the leakage inductance of the transformer than the conventional damping control.

Next, the reason why the proposed damping control has higher resonant suppression ability than the conventional damping control is discussed. The conventional damping control in the input stage has a saturation problem. Basically, the amplitude of the input current is dominated by the output power in the matrix converter. Therefore, the secondary current of the transformer command i_{2d}^* on the synchronous reference frame in Fig. 5 is set to 1 p.u. constantly in order to obtain the largest voltage transfer ratio of the system. For the conventional method, the modules operate in over modulation region because the input current commands of the modules including the damping compensation, i_{2r}^*, i_{2s}^* and i_{2t}^*, exceed 1 p.u.. Consequently, the damping effect of the conventional method is reduced due to the over modulation. Note that the voltage transfer ratio is decreased when the input current command i_{2d}^* is set under 1 p.u. in order to keep the damping effect in the conventional method. The reduction of the voltage transfer ratio is not preferred for adjustable speed drive systems. In contrast, the damping effect of the proposed control is not decreased because the matrix converter modules can control the amplitude of the output voltage within the limitation of the output voltage. From these results, the proposed damping control has higher performance than the conventional method regarding the suppression of the filter resonance.

6. Conclusion

This paper discussed the damping control to suppress the LC resonance caused by the input filter of the multi-modular matrix

converter. Past works related to the damping control for current source converters and general matrix converters have not clarified the validity for the multi-modular matrix converter. Especially, the conventional damping control applied to the input current control of the multi-modular matrix converter has two problems in terms of the number of sensors and design of the control parameters.

In this paper, a damping control suitable for the multi-modular matrix converter was proposed. The proposed damping control is combined with the output current control of the multi-modular matrix converter. Therefore, the proposed damping control suppresses the filter resonance and also diverts the output current sensors for the ACR instead of using high speed response voltage sensors on the input stage.

From simulation and experimental results, the multi-modular matrix converter without damping controls has large resonant distortion in the primary current of the transformer and the output current. However, the proposed damping control mitigates the distortion by 75.5% at steady state in experiments using the three-module model. The simulation results indicate the proposed damping control is applicable to the practical multi-modular matrix converter with nine modules. In addition, the comparison results of the damping effect between the proposed damping control and the conventional damping control are evaluated. From the THD characteristics of the primary current of the transformer which is subject to the output power, the proposed damping control suppresses the THD under 5% over 60% load region although the conventional damping control cannot reduce the THD in the region more than 90% of load. Moreover, the proposed damping control mitigates the resonant distortion under 5% in conditions of the leakage inductance from 4.71% to 14.1% while the conventional control cannot suppress the filter resonance in the region over 9.42% of the leakage inductance. Thus, the validity of the proposed damping control is confirmed by simulations and experiments. In the future, the optimal design method of the proposed damping control and the experiments with nine modules are implemented.

References

(1) P. W. Wheeler, J. Rodriguez, J. C. Clare, L. Empringham: "Matrix Converters: A Technology Review", IEEE Trans. Ind. Electron., Vol. 49, No. 2, pp. 274-288 (2002)

(2) T. Friedli, J. W. Kolar: "Milestones in Matrix Converter Research", IEEJ Journal I. A., Vol. 1, No. 1, pp. 2-14 (2012)

(3) J. Itoh, I. Sato, A. Odaka, H. Ohguchi, H. Kodachi, N. Eguchi: "A Novel Approach to Practical Matrix Converter Motor Drive System With Reverse Blocking IGBT", IEEE Trans. Power Electron., Vol. 20, No. 6, pp. 1356-1363 (2005)

(4) C. Klumpner, F. Blaabjerg, I. Boldea, P. Nielsen: "New Modulation Method for Matrix Converters", IEEE Trans. Ind. Appl., Vol. 42, No. 3, pp. 797-806 (2006)

(5) F. Blaabjerg, D. Casadei, C. Klumpner, M. Matteini: "Comparison of Two Current Modulation Strategies for Matrix Converters Under Unbalanced Input Voltage Conditions", IEEE Trans. Ind. Electron., Vol. 49, No. 2, pp. 289-296 (2002)

(6) M. Rivera, J. Rodriguez, J. Espinoza, T. Friedli, J. W. Kolar, A. Wilson, C. A. Rojas: "Imposed Sinusoidal Source and Load Currents for an Indirect Matrix Converter", IEEE Trans. Ind. Electron., Vol. 59, No. 9, pp. 3427-3435 (2012)

(7) J. W. Kolar, T. Friedli, F. Krismer, S. D. Round: "The Essence of Three-Phase AC/AC Converter Systems", Proc. 13th Power Electronics and Motion Control Conf., pp. 27-42 (2008)

(8) J. Kang, E. Yamamoto, M. Ikeda, E. Watanabe: "Medium-Voltage Matrix Converter Design Using Cascaded Single-Phase Power Cell Modules", IEEE Trans. Ind. Electron., Vol. 58, No. 11, pp. 5007-5013 (2011)

(9) E. Yamamoto, H. Hara, T. Uchino, M. Kawaji, T. J. Kume, J. K. Kang, H. P. Krug: "Development of MCs and its Applications in Industry", IEEE Industrial Electronics Magazine, Vol. 5, No. 1, pp. 4-12 (2011)

(10) J. Wang, B. Wu, D. Xu, N. R. Zargari: "Multimodular Matrix Converters With Sinusoidal Input and Output Waveforms", IEEE Trans. Ind. Electron., Vol. 59, No. 1, pp. 17-26 (2012)

(11) D. Casadei, G. Serra, A. Tani, A. Trentin, L. Zarri: "Theoretical and Experimental Investigation of the Stability of Matrix Converters", IEEE Trans. Ind. Electron., Vol. 52, No. 5, pp. 1409-1419 (2005)

(12) J. Haruna, J. Itoh: "Behavior of a Matrix Converter with a Feed Back Control in an Input Side", Proc. IEEE/IEEJ IPEC 2010, pp. 1202-1207 (2010)

(13) J. C. Wiseman, B. Wu: "Active Damping Control of a High-Power PWM Current-Source Rectifier for Line-Current THD Reduction", IEEE Trans. Ind. Electron., Vol. 52, No. 3, pp. 758-764 (2005)

(14) Y. W. Li: "Control and Resonance Damping of Voltage-Source and Current-Source Converters With LC Filters", IEEE Trans. Ind. Electron., Vol. 56, No. 5, pp. 1511-1521 (2009)

(15) Y. W. Li, B. Wu, N. R. Zargari, J. C. Wiseman, D. Xu: "Damping of PWM Current-Source Rectifier Using a Hybrid Combination Approach", IEEE Trans. Power Electron., Vol. 22, No. 4, pp. 1383-1393 (2007)

(16) M. Rivera, C. Rojas, J. Rodriguez, P. W. Wheeler, B. Wu, J. Espinoza: "Predictive Current Control With Input Filter Resonance Mitigation for a Direct Matrix Converter", IEEE Trans. Power Electron., Vol. 26, No. 10, pp. 2794-2803 (2011)

(17) J. Haruna, J. Itoh: "A Control Strategy for a Matrix Converter under a Large Impedance Power Supply", Proc. PESC 2007, pp. 659-664 (2007)

(18) T. Nunokawa, T. Takeshita:"Resonance Suppression Control in Complex Frame for Three-Phase to Three-Phase Matrix Converters", EPE2007 (2007)

(19) J. Haruna, J. Itoh: "Control Strategy for a Matrix Converter with a Generator and a Motor", Proc. 26th IEEE APEC, pp. 1782-1789 (2011)

(20) Q.Guan, P. Yang, X. Wang, X.Zhang: "Stability Analysis for Matrix Converter with Constant Power Loads and LC Input Filter", Proc. 7th IPEMC 2012, pp. 900-904 (2012)

Hiroki Takahashi

(Student member) received his B.S. and M.S. degrees in electrical, electronics and information engineering from Nagaoka University of Technology, Nagaoka, Japan in 2011 and 2013, respectively. He is currently working towards to a Ph.D. degree in electrical and electronic engineering. His research interests include matrix converters and high power conversion systems.

Jun-ichi Itoh

(Member) received his M.S. and PhD degrees in electrical and electronic systems engineering from Nagaoka University of Technology, Niigata, Japan in 1996 and 2000, respectively. From 1996 to 2004, he was with Fuji Electric Corporate Research and Development Ltd., Tokyo, Japan. Since 2004, He has been with Nagaoka University of Technology as an associate professor. He received the IEEJ Academic Promotion Award (IEEJ Technical Development Award) in 2007 and the Isao Takahashi Power Electronics Award in 2010. His research interests include matrix converters, DC/DC converters, power factor correction techniques and motor drives. He is a member of the Institute of Electrical Engineers of Japan.